Bioactive Star Gels

M. Manzano,[†] D. Arcos,[†] M. Rodríguez Delgado,[†] E. Ruiz,[†] F. J. Gil,[‡] and M. Vallet-Regí*,[†]

Departamento de Química Inorgánica y Bioinorgánica, Facultad de Farmacia, Universidad Complutense de Madrid, 28040 Madrid, Spain, and Department of Materials Science and Metallurgy, Universitat Politècnica de Catalunya, ETSEI, 08028 Barcelona, Spain

Received July 4, 2006. Revised Manuscript Received September 14, 2006

Star gels hybrid materials, suitable for use in bone repair, have been synthesized by the sol−gel method, incorporating a calcium alkoxide to the synthesis process. To determine the network connectivity and the Ca^{2+} cation location into the hybrid network, the physical and chemical properties of star gels with different compositions have been studied. In vitro bioactivity tests evidence that the star gels develop an apatite-like phase on their surface in contact with simulated body fluid, although this property depends on the Si/Ca ratio. Finally, the study of mechanical properties demonstrated that star gels are less rigid than conventional bioactive glasses, show similar fracture toughness values than cortical bone, and point to excellent long-term fatigue behavior.

Introduction

The development of new advanced materials for bone tissue repair is one of the main challenges in current developed societies.[1−3] The increase of life expectancy has led to an aging population and, consequently, to a higher incidence of bone diseases. For instance, around 40% of women older than 50 years will suffer an osteoporotic fracture.[4] This scenario requires new answers and the novel bone implants generation has shifted from tissue replacement to tissue regeneration.

Nowadays, research efforts are focused on obtaining bioactive materials able to join to bone and promote bone regeneration.[5−7] Silica-based bioactive glasses mean an extraordinary advance in this field. These materials bond to the bone tissue through the formation of an apatite-like phase on their surface when in contact with physiological fluids,[8,9] ensuring implant osteointegration. Currently, bioactive glasses are used as granulate for bone and dental grafting in small defects, or as powder incorporated into toothpaste. However, their application as pieces for medium and large defects is not possible due to their very poor mechanical properties.

In 1995, DuPont Corporation developed *star gels* materials.[10−12] Star gels are a type of organic−inorganic hybrids that present a singular structure of an organic core surrounded by flexible arms, which are terminated in alkoxysilane groups. At the macroscopic level, star gels exhibit behavior between conventional glasses and highly cross-linked rubbers in terms of mechanical properties. Currently, star gels are still one of the most interesting subjects in the field of hybrid materials.[13] The synthesis of materials able to integrate with bone and keep the mechanical properties of star gels would mean a very important advance in materials science for biomedical applications.

To the best of the authors' knowledge, this is the first time that star gels with bioactive behavior are described in the

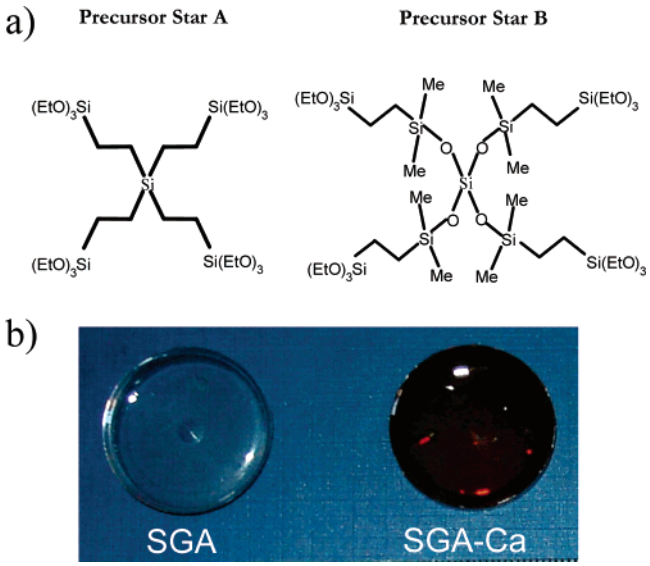

Figure 1. Molecular structure of the star gel precursors investigated (top). Transparent star gel monoliths prepared with calcium (brown monolith) and without it. The monolithic discs are 3 cm in diameter and 5 mm thick (bottom).

* Corresponding author. Fax: (+34) 91-394-1786. E-mail: vallet@farm.ucm.es.
† Universidad Complutense de Madrid.
‡ Universitat Politècnica de Catalunya.

(1) Jones, J. R.; Hench, L. L. *Curr. Opin. Solid State Mater. Sci.* **2003**, *7*, 301.
(2) Hench, L. L.; Xynos, I. D.; Polak, J. M. *J. Biomater. Sci., Polym. Ed.* **2004**, *15*, 543.
(3) Vallet-Regí, M.; Ragel, C. V.; Salinas, A. J. *Eur. J. Inorg. Chem.* **2003**, 1029.
(4) NIH Consensus Development Panel on Osteoporosis Prevention, Diagnosis, and Therapy. *JAMA* **2001**, *285*, 785.
(5) Hench, L. L.; Polak, J. M. *Science* **2002**, *295*, 1014.
(6) Arcos, D.; Greenspan, D. C.; Vallet-Regí, M. *Chem. Mater.* **2002**, *14*, 1515.
(7) Arcos, D.; Peña, J.; Vallet-Regí, M. *Chem. Mater.* **2003**, *15*, 4132.
(8) Hench, L. L.; Wilson, J. *Science* **1984**, *226*, 630.
(9) Vallet-Regí, M. *J. Chem. Soc., Dalton Trans.* **2001**, 97.
(10) Michalczyk, M. J.; Sharp, K. G. U.S. Patent 5,378,790, 1995.
(11) Sharp, K. G.; Michalczyk, M. J. *J. Sol-Gel Sci. Technol.* **1997**, *8*, 541.
(12) Sharp, K. G. *Adv. Mater.* **1998**, *10*, 1243.
(13) Sharp, K. G. *J. Mater. Chem.* **2005**, *15*, 3812.

10.1021/cm0615370 CCC: $33.50
Published on Web 11/03/2006

Table 1. Synthesis and Characterization of Star A Precursor, $Si[CH_2CH_2Si(OC_2H_5)_3]_4$

$Si(CH{=}CH_2)_4$	$HSi(OEt)_3$	^{13}C NMR (C_6D_6) in ppm:	elemental analysis;
1.3048 g	16.8595 g	3.50 ($SiCH_2$), 4.05 ($SiCH_2$),	calcd for $C_{32}H_{76}Si_5O_{12}$ (wt %), C 48.4, H, 9.65;
(0.0095 mol)	(0.1025 mol)	18.4 (CH_3), 58.4 ($SiOCH_2$)	found, C 45.5, H 9.02

Table 2. Synthesis and Characterization of Star B Precursor, $Si[OSi(CH_3)_2CH_2CH_2Si(OC_2H_5)_3]_4$

$(CH_2{=}CH)Si(OEt)_3$	$Si[OSi(CH_3)_2H]_4$	^{13}C NMR (C_6D_6) in ppm:	elemental analysis; calcd for $C_{40}H_{100}Si_9O_{16}$ (wt %),
10.024 g	3.039 g	0.10 ($Si(CH_3)$), 3.12 ($SiCH_2$),	C 44.1, H 9.25;
(0.05278 mol)	(0.0092 mol)	10.2 ($SiCH_2$), 18.4 (CH_3), 58.3 ($SiOCH_2$)	found, C 44.4, H 8.90

Table 3. Reactant Amounts for the Synthesis of Bioactive star gels

sample	Star A precursor	Star B precursor	Ca(OR)(OR′)	HCl (1 N) (mL)	EtOH (mL)
SGA	1.9 g (2.4 mmol)			0.05	2.4
SGA-Ca	3.17 g (4 mmol)		3.8 g (4 mmol)	0.10	5.0
SGA-2Ca	1.59 g (2 mmol)		3.8 g (4 mmol)	0.05	2.5
SGB		1.72 g (1.6 mmol)		0.04	1.6
SGB-Ca		4.36 g (4 mmol)	3.8 g (4 mmol)	0.10	4.0
SGB-2Ca		1.72 g (1.6 mmol)	3.0 g (3.16 mmol)	0.04	1.6

scientific literature. These materials can be excellent candidates for bone tissue regeneration if several conditions are satisfied: (a) star gels must be obtained as monoliths of different shapes to fit to any kind of medium or large bone defect; (b) star gels must be structurally homogeneous to predict their biological and mechanical response when implanted; (c) star gels must be able to develop an apatite-like phase in contact with physiological fluids, i.e., must be bioactive; and (d) star gels must exhibit mechanical properties significantly better than those exhibited by conventional bioactive glasses.

In this article, the synthesis method that leads to the obtainment of these materials is described. Also, an effort to understand these new materials from different points of view (chemical, structural, biological, and mechanical) has been carried out.

Experimental Section

Bioactive star gels (BSGs) were obtained by hydrolysis and condensation of the precursors plotted in Figure 1a into network structures. The precursors were synthesized from platinum-catalyzed hydrosilylation reactions, i.e., addition reactions between Si−H and C═C groups in the presence of a catalyst. The precursors syntheses are described elsewhere,[10] and ^{13}C NMR spectra and elemental analysis were performed to assess the product purity. These results are collected in Tables 1 and 2 for Star A and Star B precursors, respectively.

In this work we have developed new star gels by incorporation of calcium alkoxide during the polycondensation process of the precursors. The stoichiometric amounts for the different star gels obtained are collected in Table 3. In a typical synthesis, 3.17 g (4 mmol) of Star A precursor and 3.8 g (4 mmol) of calcium methoxy ethoxyde were dissolved in 5 mL of anhydrous ethanol together with 0.1 mL of aqueous HCl (1 N) under argon atmosphere. The water:precursor molar ratio was calculated to be 12. After 1 week at room temperature, the sol was aged at 60 °C for 4 weeks and dried for a week at 90 °C. After this process, homogeneous transparent monoliths were obtained (Figure 1b). Six different star gels are presented here. SGA and SGB do not contain calcium. SGA-Ca and SGB-Ca have a molar ratio Ca/precursor equal to 1. Finally, SGA-2Ca and SGB-2Ca have a molar ratio Ca/precursor equal to 2.

For comparison purposes, traditional SiO_2−CaO sol−gel bioactive glasses were synthesized. Following the same process described above, tetraethyl orthosilicate (TEOS) was added as an SiO_2 source together with calcium methoxyethoxyde in stoichiometric amounts to obtain 90:10 SiO_2:CaO and 80:20 SiO_2:CaO (mol %). These sol−gel glasses possess a Si/Ca ratio similar to that of SGA-Ca and SGA-2Ca, respectively.

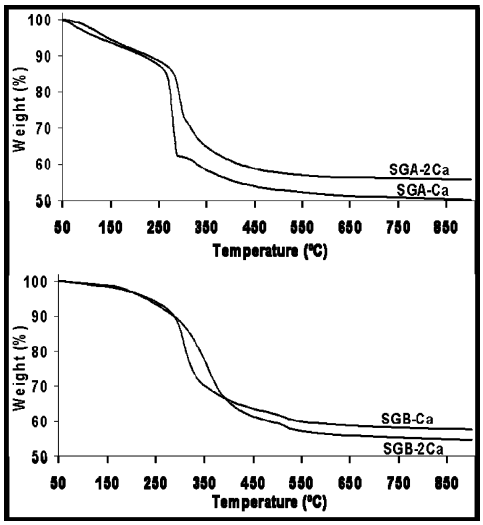

Figure 2. TG analyses of the synthesized star gels.

Thermogravimetric (TG) analyses were carried out with a Pyris Diamond TG/DTA instrument, under air atmosphere with a heating rate of 5 °C·min^{-1}.

Fourier transformed infrared spectroscopy (FTIR) was carried out with a Nicollet Nexus spectrometer from 500 to 4000 cm^{-1} using KBr technique and operating in the transmittance mode.

Powder X-ray diffraction (XRD) experiments were performed with a Philips X'Pert diffractometer by using Cu Kα radiation. Patterns were collected with a step size of 0.04° 2θ and 5 s of counting time.

Solid state ^{29}Si cross-polarized (CP) NMR spectroscopy was used to measure the degree of condensation (extent of reaction) in the gels by the relative abundance of trifunctional silicon nuclei from terminal R−Si sites. MAS NMR spectra were performed on a Bruker Advance-400 WB spectrometer at 79.49 MHz.

Assessment of in vitro bioactivity was carried out by soaking the star gels monoliths in 40 mL of filtered simulated body fluid (SBF) in polyethylene containers at 37 °C under sterile conditions. SBF has similar composition and ionic concentrations to those of human plasma.[14] Concentrations of Ca as well as pH levels of the

(14) Kokubo, T.; Kushitani, H.; Sakka, S.; Kitsugi, T.; Yamamuro, T. *J. Biomed. Mater. Res.* **1990**, *24*, 721.

Table 4. Assignation of FTIR Absorption Bands for SGA, SGA-Ca, and SGA-2Ca Samples[a]

SGA ν (cm^{-1})	SGA-Ca ν (cm^{-1})	SGA-2Ca ν (cm^{-1})	mode	structural units
3700−3000 (m, br)	3700-3000 (m, br)	3700-3000 (m, br)	OH,H	OH envelope
2975 (m)	2976 (m)	2975 (m)	ν_{as}(C−H)	$-CH_2-R$
2922 (m)	2926 (m)	2922 (m)	ν_{as}(C−H)	$-CH_2-R$
2898 (m)	2883 (m)	2898 (m)	ν_{s}(C−H)	$-CH_2-R$
2884 (m)	2830 (m)	2884 (m)	ν_{s}(C−H)	$-CH_2-R$
1635 (w, br)	1635 (w, br)	1635 (w, br)	δ(H−O−H)	H_2O
1460 (w)	1456 (w)	1450 (w)	2ν(Si−C)	$\equiv Si-CR_2-$
	1197 (m, sh)	1199 (m, sh)	ν(Si−O−C)	$\equiv Si-O-CH_2-CH_3$
1150 (m, sh)	1160 (m, sh)	1150 (m, sh)	ν(Si−C)	$\equiv Si-CH_2-CH_2-Si\equiv$
1100 (s, sh)	1098 (s, sh)	1099 (s, sh)	ν_{as}(Si−O−Si)	$\equiv Si-O-Si\equiv$
1024 (s, br)	1036 (s, br)	1032 (s, br)	ν_{as}(Si−O−Si)	$\equiv Si-O-Si\equiv$
952 (w, sh)	952 (w, sh)	954 (w, sh)	ν(Si−OH)	$\equiv Si-OH$
875 (w)	843 (w)	842 (w)	r(Si−C)	$\equiv Si-CR_2-$
730 (m, br)	763 (m, br)	764 (m, br)	ν_{s}(Si−O−Si)	$\equiv Si-O-Si\equiv$
675 (w)	672 (w)	669 (w)	ν_{s}(Si−C)	$\equiv Si-CR_2-$
440 (s)	432 (s)	430 (s)	δ(Si−O−Si)	−O−Si−O−

[a] w = weak, m = medium, s = strong, sh = sharp, br = broad.

Table 5. Assignation of FTIR Absorption Bands for SGB, SGB-Ca, and SGB-2Ca Samples

SGB ν (cm^{-1})	SGB-Ca ν (cm^{-1})	SGB-2Ca ν (cm^{-1})	mode	structural units
3700−3000 (m, br)	3700−3000 (m, br)	3700−3000 (m, br)	OH,H	OH envelope
2957 (m)	2957 (m)	2954 (m)	ν(C−H)	$-CH_2-R$
2923 (m)	2925 (m)	2925 (m)	ν(C−H)	$-CH_2-R$
2895 (m)	2895 (m)	2898 (m)	ν(C−H)	$-CH_2-R$
2879 (m)	2879 (m)	2878 (m)	ν(C−H)	$-CH_2-R$
2850 (sh)	2820 (sh)	2834 (sh)	ν(C−H)	$-CH_2-R$
1739 (w)	1735 (w)	1735 (sh)	δ(H−O−H)	H_2O
1408 (w)	1408 (w)	1426 (m)	δ_{as}(Si−CH_3)	$\equiv Si-CH_3$
1251 (m)	1251 (m)	1251 (m)	δ_{s}(Si−CH_3)	$\equiv Si-CH_3$
1170 (w, sh)	1200 (w, sh)	1201 (w)	ν(Si−O−C)	$\equiv Si-O-CH_2-CH_3$
1145 (m, sh)	1140 (m, sh)	1140 (m, sh)	ν_{as}(Si−O−Si)	$\equiv Si-O-Si\equiv$
1115 (m, sh)	1102 (m, sh)	1094 (m, sh)	ν_{as}(Si−O−Si)	$\equiv Si-O-Si\equiv$
1070 (m, sh)	1071 (m, sh)		ν(Si−O−C)	$\equiv Si-O-CH_2-CH_3$
1020 (s, br)	1028 (s, br)	1024 (s, br)	ν_{as}(Si−O−Si)	$\equiv Si-O-Si\equiv$
964 (m, sh)	959 (m, sh)	948 (m, sh)	ν(Si−OH)	$\equiv Si-OH$
832 (s)	835 (s)	835 (s)	r(Si−C)	$\equiv Si-CR_2-$
777 (s)	777 (s)	780 (s)	ν_{s}(Si−C)	$-Si(CH_3)_2-O-$
420 (s)	420 (s)	425 (s)	δ(Si−O−Si)	−O−Si−O−

solutions after soaking of the materials were determined using an Ilyte $Na^+K^+Ca^{2+}$ pH system. Surface morphology was studied by scanning electron microscopy (SEM) in a JEOL 6400 microscope. Transmission electron microscopy (TEM) was carried out on a JEOL JEM-3000F microscope equipped with an ISIS 300 X-ray microanalysis system (Oxford Instruments) with a LINK "Pentafet" detector for EDX analyses. To study the modifications that occur on the surface of the specimens, the samples for TEM experiments were prepared by gently scratching from the surface of the specimens. The powder so obtained was dispersed in acetone and placed onto copper grids.

Mechanical properties were determined by indentation techniques. Compressive strength values were obtained by means of a MTS nanoindenter. Around 80−90 indentations were carried out on the star gel disks (15 mm in diameter and 3 mm thickness). The MTS nanoindenter system records the material displacement as a function of the applied strength to calculate the compressive strength. Fracture toughness (K_{Ic}) values were determined by means of a Matzuzawa microhardness tester with Vickers and Knoop indenters.

Results and Discussion

As a result of the synthesis process, transparent crack-free monoliths, which have copied the shape of the reaction vessel, were obtained (see Figure 1b). The procedure described above allows tailoring of the shape and size of the monoliths by using vessels with different shapes and/or changing the amounts of reactants.

The BSGs were chemically characterized by TG analyses and FTIR spectroscopy. TG analyses for calcium-containing star gels are shown in Figure 2. TG patterns show around 45% of weight loss between 270 and 300 °C, corresponding to the decomposition of the organic component, $-CH_2-CH_2-$. SGB-Ca and SGB-2Ca showed an additional small weight loss (around 1−2%) at 530 °C. Taking into account that silicones typically decompose at temperatures around 530 °C, this small weight loss can be assigned to the $-Si-CH_3$ groups decomposition of the SGB internal structure. The FTIR spectra showed the typical absorption bands corresponding to the expected functional groups (see Tables 4 and 5).

As mentioned before, star gels are organic−inorganic hybrid materials resulting from the hydrolysis and polycondensation of the alkoxysilane groups, located at the end of the precursor arms. However, it is mandatory to know how Ca^{2+} is incorporated into the hybrid network to understand the possible bioactive behavior of these materials. For this purpose, ^{29}Si CP-MAS NMR spectroscopy (Figure 3) was used to measure the degree of condensation (extent of reaction) in the gels by the relative abundance of trifunctional silicon nuclei from terminal R−Si sites. Trifunctional silicon

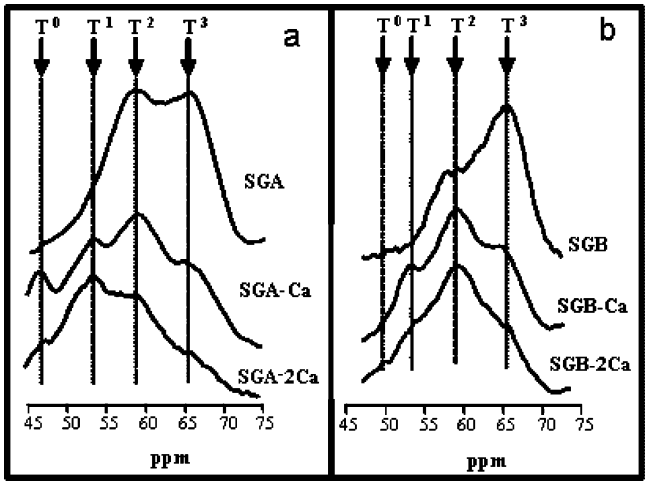

Figure 3. (a) ^{29}Si CP-MAS NMR spectra of star gels obtained from precursor Star A and (b) precursor Star B.

centers were named with the conventional T^n notation, where T refers to $(SiO)_nR'Si(OR)_{3-n}$ units and n to the number of bridging oxygen atoms surrounding the central silicon atom. In both BSG materials, the T^2, T^1, and T^0 relative contribution was observed to increase as the amount of Ca^{2+} introduced into the hybrid network was enlarged. The percentage of T^3 species was decreased when Ca^{2+} was added due to the role of Ca^{2+} in the network, i.e., reducing the cross-linking density and, therefore, reducing the amount of fully condensed Si−O−Si structures. Although the T^2, T^1, and T^0 contribution are also produced by the presence of the Si−OH groups, there is a close relationship between the Ca content and the network connectivity. These results point out that the Ca^{2+} cations would be incorporated into the inorganic silica domain of the star gel network, in a similar way that Ca^{2+} cations incorporate into the conventional bioactive sol−gel glasses.

XRD experiments, Figure 4, showed the characteristic patterns of amorphous materials in all cases. These results demonstrate that crystalline phase aggregation does not occur when Ca is incorporated into the star gel network.

The bioactivity evaluation was carried out by soaking the star gel monoliths in SBF at 37 °C. In general, bioactive materials such as conventional bioglasses develop an apatite-like phase when soaked in this solution, and it is widely accepted that these materials will do the same under in vivo conditions. The subsequent bioactive bond between bone and implant will be formed through this new apatite phase.[15]

Figure 5 shows the pH and the Ca^{2+} content in SBF as a function of monoliths soaking time. Ca^{2+} ions are released to the SBF during the first hours in the case of SGA-Ca, SGA-2Ca, and SGB-2Ca, whereas the Ca^{2+} content of SBF is not significantly modified in sample SGB-Ca. During the first hour a significant pH increase occurs, following the same trend as the Ca^{2+} variation.

The Ca^{2+} released to SBF and the increase of pH in samples SGA-Ca, SGA-2Ca, and SGB-2Ca are in agreement with the mechanism proposed by Kokubo for apatite formation on the surfaces of bioactive silica-based glasses.[16] In such glasses, an exchange between Ca^{2+} ions of the glass and H^+ of the solution takes place. This gives rise to the formation of Si−OH groups on the surface, inducing apatite nucleation.

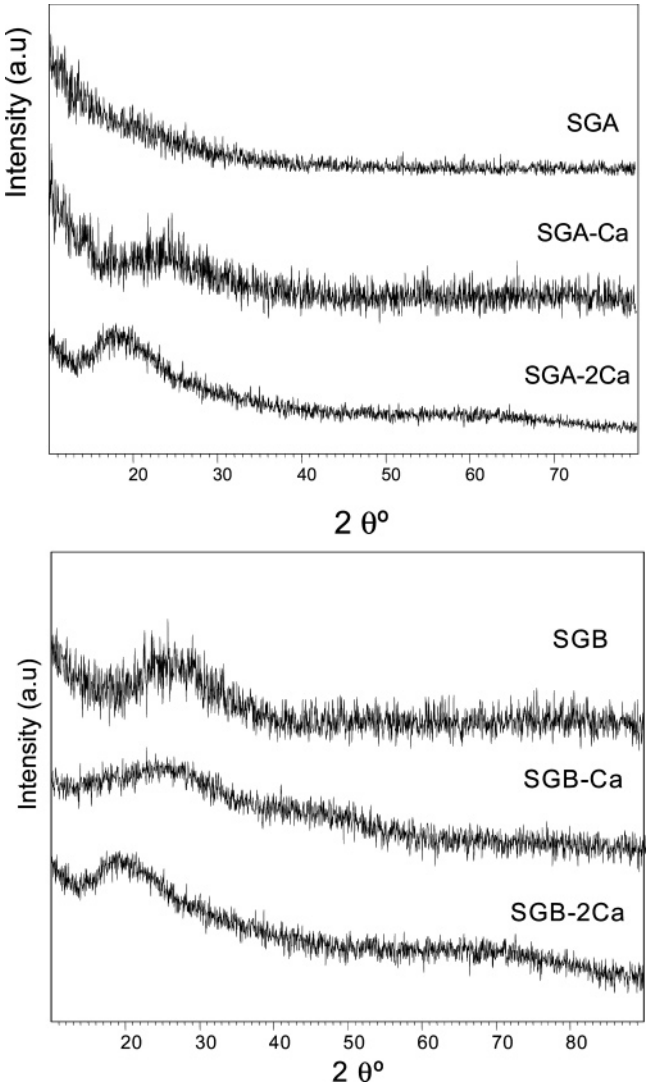

Figure 4. X-ray diffraction patterns of all the star gels studied. Noncrystalline phase can be observed.

Figure 6 shows the scanning electron micrographs for sample SGA-Ca before and after soaking in SBF for 7 and 17 days. Before soaking, the micrograph shows a smooth surface characteristic of a nonporous and homogeneous gel. Also, EDX spectroscopy confirms the presence of Si and Ca as the only components of the inorganic phase. After 7 days, a new phase can be clearly observed. This new phase partially covers the star gel surface. A higher micrograph magnification reveals that it is formed by rounded submicrometer particles. The EDX spectroscopy indicates that the Ca and P contents increase with respect to the Si, pointing out that this new phase is composed of a calcium phosphate. The micrograph of the star gel after 17 days shows the monolith surface fully covered by a layer constituted of spherical particles. A higher magnification shows that these

(15) Hench, L. L.; Anderssson, O. In *Bioactive Glasses. An introduction to Bioceramics*; Hench, L.L., Wilson, J., Eds.; Elsevier Science: New York, 1995; p 477.

(16) Kokubo, T.; Kushitani, H.; Ohtsuki, C.; Sakka, S.; Yamamuro, T. *J. Mater. Sci. Mater. Med.* **1992**, *3*, 79.

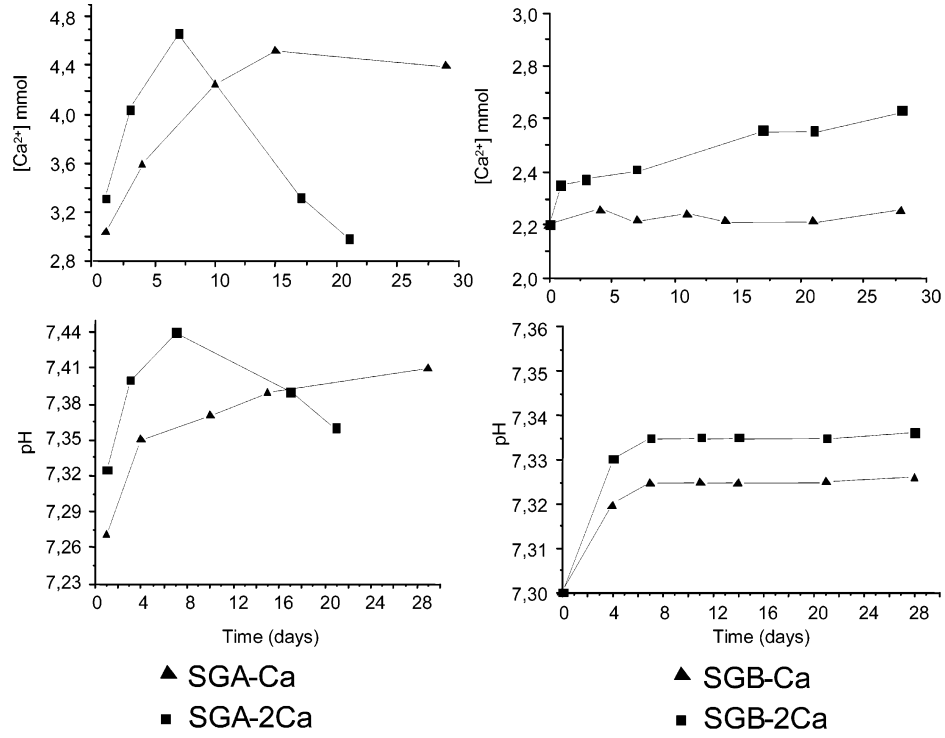

Figure 5. Calcium concentration and pH evolution of the SBF as a function of star gels soaking time.

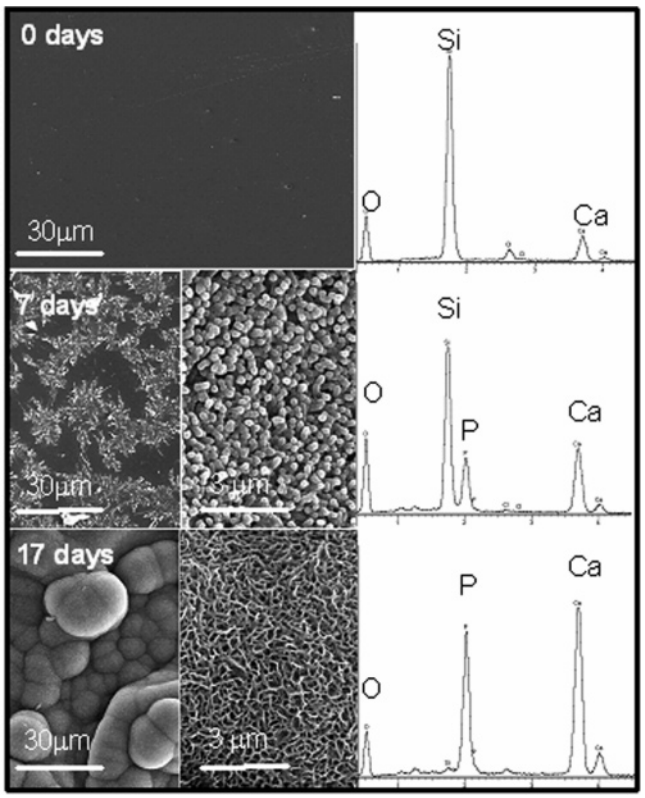

Figure 6. SEM micrographs and EDX spectra of the SGA-Ca surface before and after being soaked in SBF. EDX spectra clearly show the evolution of the inorganic chemical composition on the surface: from silicon and calcium oxide to a calcium phosphate.

particles are aggregates of numerous needle-shaped crystallites, which are characteristic of the apatite phase growth over bioactive materials surfaces.[17,18] The EDX spectrum indicates that, at this point, the surface is fully covered by a calcium phosphate with a Ca/P ratio of 1.6 (very similar to 1.67 for stoichiometric hydroxyapatite).

The structural homogeneity of SGA-Ca and the formation of a nanocrystalline apatite phase on their surface have been further demonstrated by HRTEM microscopy. Figures 7a and 7c show the HRTEM image of SGA-Ca before soaking in SBF and the corresponding electron diffraction (ED) patterns (Figure 7a, inset).

The images show the typical contrast of an amorphous material and the ED pattern shows a broad diffused scattering, which is indicative of the amorphous nature. These results confirm the amorphous structure of the bioactive star gels. EDX analyses evidence the presence of Ca taking part of the chemical composition at a surface level. From a semiquantitative point of view, the EDX analyses provided Si/Ca ratio values very close to the theoretical ones. Figures 7b and 7d were obtained after soaking the SGA-Ca for 3 weeks in SBF. The images were collected from the surface of the star gels. For this purpose, some particles were gently scratched from the surface monoliths. TEM images show crystalline domains, where oriented planes can be easily distinguished (Figure 7d). The EDX spectra collected from these areas show chemical compositions that would correspond to those expected for an apatite-like phase, that is, Ca and P as main components. The ED patterns colleted from these particles correspond to a typical polycrystalline material (Figure 7b, inset). The interplanar spacings of the rings observed correspond to the (002), (211), and (222) reflections of an apatite-like phase.

To determine the compositions for which star gels are bioactive, these experiments have been carried out for SGA,

(17) Vallet-Regí, M.; Arcos, D.; Pérez-Pariente, J. *J. Biomed. Mater. Res.* **2000**, *51*, 23.

(18) Izquierdo-Barba, I.; Salinas, A. J.; Vallet-Regí, M. *J. Biomed. Mater. Res.* **1999**, *47*, 243.

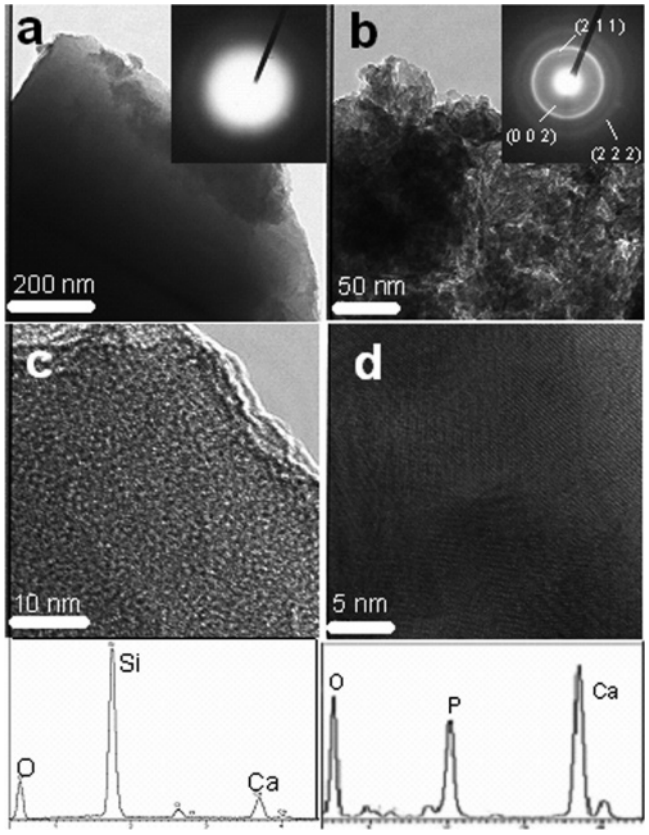

Figure 7. HRTEM images of SGA-Ca before soaking in SBF (a) and after 3 weeks in SBF (b). Images (c) and (d) are magnifications of (a) and (b), respectively. The insets in (a) and (b) are the ED patterns acquired during the observations. EDX spectra before soaking (bottom-left) and after soaking for 3 weeks in SBF (bottom-right) confirm the surface evolution during the bioactive process.

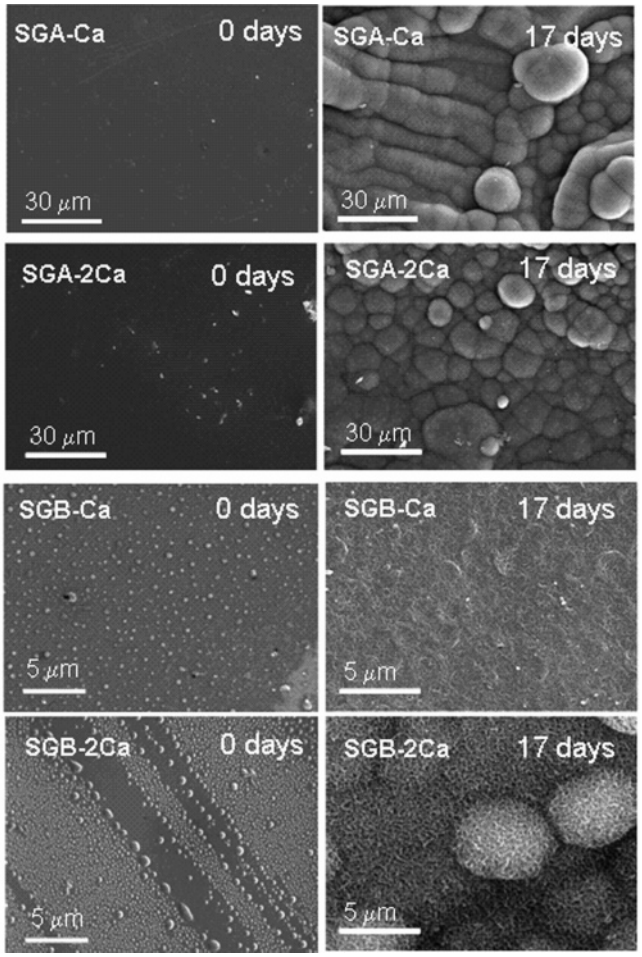

Figure 8. Bioactivity tests followed by SEM. Star gels obtained from Star precursor A develop an apatite-like phase when soaked in SBF. Star gel SGB-Ca with a Si/Ca molar ratio of 9 does not develop apatite at the surface. SGB-2Ca with a Si/Ca ratio of 4.5 exhibits in vitro bioactivity.

SGA-Ca, and SGA-2Ca (with precursor star A) and SGB, SGB-Ca, and SGB-2Ca. Figure 8 collects the SEM micrographs after 17 days in SBF for the samples prepared with calcium. The evolution of the surface morphology shows that only SGA-Ca, SGA-2Ca, and SGB-2Ca are bioactive, whereas star gels without Ca and SGB-Ca are not (micrographs not shown). The explanation rests on the network connectivity of the different star gels. The molar ratios Ca: star gel precursors are the same for SGA-Ca (bioactive) as for SGB-Ca (non-bioactive), i.e., equal to 1. However, every SGB precursor molecule has nine silicon atoms, whereas every SGA precursor molecule has only five. These results indicate that the star gels Si/Ca molar ratio must be around 9 or lower to be bioactive. Otherwise, the amount of network modifier, i.e., Ca^{2+}, is not enough and the star gel is too stable to react with physiological fluids. It must be taken into account that the bioactive process starts with the ionic exchange between Ca^{2+} from the network and H^{+} from the fluids.[15]

The bioactive star gels monoliths exhibit substantially better mechanical behavior than conventional glasses. Figure 9 shows the nanoindentation values carried out over numerous sites of the tested materials. In general, the mechanical properties values showed very low standard deviations, which affirms that the bioactive star gels are chemically homogeneous.

Figure 9a shows the nanohardness values for different star gels and conventional sol−gel glasses monoliths with analogous chemical compositions. It can be seen that the maximum value is shown by the conventional sol−gel glass (90Si10Ca), whereas star gels are softer. Figure 9a indicates that the presence of the organic chains result in softer materials in such a way that the longer the organic component (SGB-2Ca), the lower the hardness values.

These results are in agreement with Young's modules calculated (Figure 9b). Conventional sol−gel glass also evidences the highest value, followed by SGA-Ca and SGB-2Ca. The Young's module is a material constant that mainly depends on the chemical bond elastic forces. In the case of conventional sol−gel glasses, chemical bonds undergo very little deformation under a mechanical load, mainly due to their high bond energy that leads to rigidity and, consequently, very small deformations. The organic component addition results in an averaged bond stiffness decreasing (produced by this new more flexible geometrical configuration). In this case, the elastic deformation is higher under the same mechanical load. At this point, it is clear that SGB-2Ca shows a very low Young's module and, therefore, it is not an appropriate material for structural purposes. However, SGA-Ca material shows a Young's module very similar to cancellous bone (0.5−1.5 GPa) and lower compared to cortical bone (4−10 GPa).[19]

(19) Currey, J. D. *J. Biomech.* **1998**, *21*, 131.

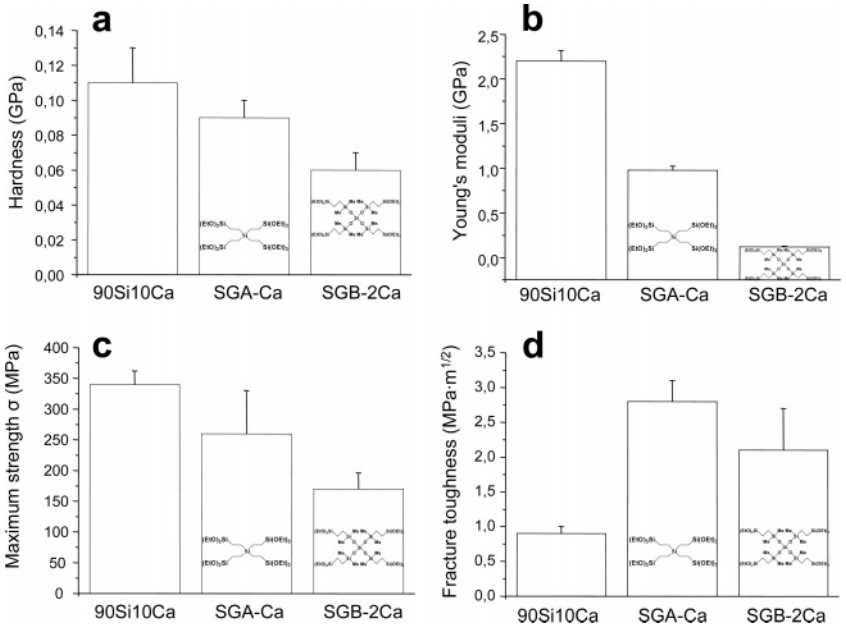

Figure 9. Mechanical parameters calculated by nanoindentation tests for conventional sol−gel glass (90Si10Ca) and two different bioactive star gels with analogous Ca/Si molar ratio. For better understanding, the precursor structures are also included. (a) Hardness values, (b) Young's modules, (c) maximum strength (σ), and (d) fracture toughness of the same samples. Values are represented as the average of multiple tests with the corresponding standard deviation.

By calculating the compressive maximum strength (σ) values, we can observe the same trend for the Young's modules and hardness (Figure 9c). It should be noted that these values are an approximation to the true values, as the samples shapes were not normalized. The configuration influence in SGB-2Ca is clearly observed, where the strain at maximum strength deformation is higher compared with those of the other samples. This fact could be explained by the chemical bonds deformability in SGB-2Ca. It could be observed that the fracture deformation values were around 0.25% and 0.70% for 90Si10Ca and SGB-Ca, respectively. It means that there is no energy absorption before breaking and the fracture can be considered as fragile.

Fracture mechanics describes the fracture process in a material by relating the stress field close to the crack tip with the resultant extension of the crack length. This allows description of the resistance of a material to rapid crack propagation in terms of a basic parameter: the critical stress intensity factor (K_{Ic}) also known as fracture toughness. Fracture toughness values of star gels are significantly higher than conventional sol−gel glasses (Figure 9d). It means that star gels are able to absorb more energy before breaking. Fracture toughness is a very important value when considering materials for clinical applications.

As could be expected, conventional sol−gel glass is the material with the lowest K_{Ic} value, whereas the organic−inorganic hybrid materials show a significant increment of this value. The more flexible structure of star gels allows rotation and deformations that result in materials with better toughness than conventional sol−gel glasses. In fact, K_{Ic} values for star gels fall into the same order of magnitude of K_{Ic} values for cortical bone determined by several authors (see Table 6).

Table 6. Fracture Toughness (K_{Ic}) Values of the Conventional Sol−Gel Glass, Star Gels, and Those Obtained for Human Cortical Bone by Different Authors

specimen	direction	K_{Ic} (MPa·m$^{1/2}$)	reference
90Si10Ca	N/A	0.8	
SGA-Ca	N/A	2.8	
SGB-2Ca	N/A	2.1	
human tibia	longitudinal	2.4−5.3	20
human tibia	longitudinal	3.7	21
human femur	transversal	6.4	22

The structural effects of the materials produce a strong influence on the fracture toughness, so this explains the difference of the K_{Ic} values between the star gels investigated here (Figure 9d). SGB-2Ca structure presents more Si−O−Si covalent bonds than SGA-Ca, which means that the SGB-2Ca structure would tend to propagate more a pre-existing crack than SGA-Ca structures. This structural difference between SGA-Ca and SGB-2Ca is not so important in the rest of the mechanical parameters (hardness, Young's modules, and compressive strength) because they are not as sensitive to the differences between structural chains.

Finally, a preliminary fatigue test has been carried out by means of cyclic loading with a nanoindentor. Bone is repeatedly cyclically stressed and fatigue is one of the causes of bone failure reported in the literature.[23] Under a 40 MPa stress force, a human femur shows between 100 and 125 cycles to fracture. Our star gels resisted more than 250 cycles, whereas the conventional sol−gel glass, 90Si10Ca, resisted only around 30 cycles. From these results, star gels are expected to exhibit good long-term fatigue behavior.

(20) Bonfield, W.; Behiri, J. C.; Charambilides, B. In *Biomechanics: Current Interdisciplinary Research*; Perrin, S. M., Scheider, E., Eds.; Martinus Nijhoff: Dordrecht, The Netherlands, 1984; p 36.
(21) Norman, T. L.; Vashischth, D.; Burr, D. B. *J. Biomech.* **1995**, *28*, 309.
(22) Zioupos, P.; Currey, J. D. *Bone* **1998**, *22*, 57.
(23) Krause, J. R.; Thompson, J. R. *Am. J. Roentgenol.* **1994**, *52*, 281.

Conclusions

Bioactive star gels can be obtained as monoliths of any shape and size and are able to develop an apatite phase on their surface when soaked in SBF. These bioactive star gels are homogeneous and substantially better than conventional bioactive glasses from a mechanical point of view. Therefore, bioactive star gels are excellent candidates for osseous regeneration in medium and large bone defects.

Acknowledgment. Financial support of CICYT Spain, through research projects MAT2005-01486 and CAM S-0505/MAT/000324, is acknowledged. D.A. is grateful to MEC for the financial support through the "*Ramón y Cajal*" postdoctoral grant.

CM0615370